J. Environ. Nanotechnol.
Volume 3, No.4 (2014) pp. 41-53
ISSN (Print): 2279-0748
ISSN (Online): 2319-5541
doi: 10.13074/jent.2014.12.143109

Photocatalytic Decolorization of Textile Effluent by using Synthesized Nano particles

Narayanappa Madhusudhana[1], Kambalagere Yogendra[1*], Kittappa M. Mahadevan[2]

[1*]*Department of P.G studies and Research in Environmental Science, Kuvempu University, JnanaSahyadri, Shankaraghatta, Shivamogga, Karnataka, India.*
[2]*Department of Chemistry, Kadur P.G Center, Kuvempu University, Kadur, Karnataka, India.*

Received: 08.10.2014 Accepted: 03.11.2014

Abstract

The textile industry consumes considerable amounts of water during the dyeing and finishing operations. Dyes extensively used are found to be toxic and considered to be resistant to biodegradation. In this work, a detailed investigation was done on photocatalytic degradation for selected textile effluent. The two different nano particles, $CaAl_2O_4$-I was synthesized by using fuel urea and $CaAl_2O_4$-II by acetamide by solution combustion method. These nano particles were characterized by using X-ray diffraction (XRD), Scanning Electron Micrograph (SEM) and UV absorbance spectroscopy. The average size was found to be 39 nm for $CaAl_2O_4$-I and 42 nm for $CaAl_2O_4$-II. The band gap of the nano particle $CaAl_2O_4$-I was found to be 2.8 eV and $CaAl_2O_4$-II was 2.7 eV. These nano particles were tested for the photocatalytic degradation by varying parameters such as catalyst concentration, pH and dye concentration. Also, the efficiency of the synthesized nano particles were compared with the procured TiO_2 of size < 25 nm.

Keywords: *$CaAl_2O_4$; Degradation; Nano particles; Photocatalyst; Textile effluent; TiO_2.*

1. INTRODUCTION

Dyes are being the most used coloured products in textile industries. These reactive dyes are not easily removable by conventional treatment methods due to their stability and non biodegradable nature. The coloured wastewaters released by textile industry effluent pose a potential environmental hazard to ecosystem and must be treated before being discharged into the natural water bodies. Until now there is no such economical and technically fit solution for the effective degradation and mineralization of the hazardous, organic compounds present in textile industry effluents is available. Various methods like physical, biological and chemical are being explored and employed however they have their own limitations as the physical methods like adsorption on activated carbon, reverse osmosis etc. do not lead to complete mineralization, rather they simply transfer the pollutants from one phase to another causing secondary pollution (Manjusha and Pragati, 2014; Madhusudhana *et al.* 2013). Biological treatment methods have proven to be ineffective not only due to the resistance of azo dyes to aerobic degradation (Mohammad *et al.* 2005) but also due to the formation of aromatic amines which are carcinogenic (Swati *et al.* 2012).

Therefore from the last decade, focus has been mainly on the treatment technologies that lead to the complete destruction of the dye molecules. Among these treatments advanced oxidation processes (AOPs) has emerged as a powerful remediation treatment to destroy refractory pollutants in water. Among all the AOPs heterogeneous photocatalysis has been found to be the most promising treatment process for the degradation of various dyes at lab scale (Malato *et al.* 2002). But to extend this process to treat real textile industrial effluent, more focused and detailed study is the need of current research and development activities. Also it is so advantageous that, its ability to photosensitize the complete mineralization of widerange of organic pollutants without production of harmful by-products.

***Kambalagere Yogendra** Tel.no:+919945352191
E-mail: madhubdvt@gmail.com*

Among the metal oxide photocatalysts, TiO_2 is the most studied nano particle and frequently reported as an efficient photocatalyst in degrading many textile dyes. Many investigations have been carried out under UV radiation, since TiO_2 photocatalysts show relatively high activity and chemical stability under UV light (Yeber *et al*. 2000) and absorbs only small portion of solar spectrum in the UV region. On the other hand, ZnO has approximately the same band gap energy (3.2 eV) as TiO_2 and its photocatalytic capacity has been anticipated to be similar to that of TiO_2. Further, some studies have confirmed that ZnO exhibits more efficiency than TiO_2. The biggest advantage of ZnO is that, it absorbs over a larger fraction of the solar spectrum than TiO_2 (Behnajady *et al.* 2006; Lizama *et al.* 2002; Khodja *et al.* 2001; Gouvea *et al*. 2000). Similar studies have reported in our laboratory on different dyes (Madhusudhana *et al.* 2012; Madhusudhana *et al.* 2012; Gopalappa *et al.* 2012; Gopalappa *et al.* 2012; Madhusudhana *et al.* 2011; Yogendra *et al.* 2011).

So, in continuation of our study, TiO_2 of Size < 25 nm has been procured from sigma Aldrich and compared with the two different synthesized $CaAl_2O_4$ nano particles. The nano particle was characterized by X-ray diffraction (XRD)and Scanning Electron Micrograph (SEM) studies. The decolorization of one of the textile effluent solution (3%) was experimented in presence of sunlight irradiation.

2. EXPERIMENTAL DETAILS

2.1 Materials and Reagents

The TiO_2 nano particle of size < 25 nm was procured from sigma-aldrich, Mumbai. $CaAl_2O_4$-I and $CaAl_2O_4$-II nano particles were synthesized in the laboratory by $Ca(NO_3)_2.4H_2O$ and $Al(NO_3)_3.9H_2O$ using fuels urea and acetamide, because they seem to be the convenient fuels which are easily available for the synthesis of the $CaAl_2O_4$ nano particles. The coloured textile effluent was collected form one of the nearby textile industries. The chemicals like calcium nitrate $Ca(NO_3)_2.4H_2O$ (99%, AR), aluminium nitrate $Al(NO_3)_3.9H_2O$ (99%, A. R.), urea (NH_2 CO NH_2) (99%, AR) and acetamide (CH_3CONH_2) (99%, AR) were obtained from Hi-media chemicals, Mumbai and used as received. The UV-VIS single beam spectrophotometer 119 (Systronics) has been used for recording absorbance at λ_{max}.

2.2 Synthesis of calcium aluminate nano particle by solution combustion method

The solution combustion process is an exothermic redox (oxidation and reduction reactions taking place simultaneously) reaction between an oxidizer and a fuel. When the heat is more evolved than the heat required for the reaction, the system becomes self-sustained. Also the exothermicity of such reactions takes the system to a high temperature. Hence, this process, popularly known as self-propagating high temperature synthesis, which is also called fire synthesis. The interesting feature of the process is that the sample once ignited continues to burn to consume itself (Mimani and Patil, 2001).

The stoichiometry or the equivalence ratio (ϕ_e, O/F), at which the total combustion reaction takes place is very important and crucial. Combustion may not take place at all if the stoichiometry is not maintained. The calculation of the equivalence ratio is based on balancing the oxidizing (O) and reducing valency (F) of the reactants. The energy released by the combustion of the redox mixtures will be maximum when the equivalence ratio is (ϕ_e, O/F), unity (O is the total oxidizing and F the total reducing valency of the components). Here, the elements C, H and metal ions are considered as reducing species (e.g., C = +4, H = +1, M^{2+} = +2, M^{3+} = +3, etc.). Oxygen is considered as oxidizer with a valency of –2. Nitrogen is considered to have zero valency (Deshpande *et al*. 2004).

2.2.1 Synthesis of $CaAl_2O_4$-I

The stoichiometric amounts of $Ca(NO_3)_2.4H_2O$ (3.54g) and $Al(NO_3)_3.9H_2O$ (11.255g) were dissolved in minimum quantity of water along with Urea (24g) in a silica crucible (with volume of 100 cm^3). The resulting mixture was introduced into the muffle furnace which was preheated to 600°C. Initially the solution foils boils and undergoes dehydration followed by decomposition with the evolution of gases (N_2 and CO_2). Then, it burns to yield voluminous and foamy homogeneous residue (Nesaraj *et al*. 2007). Thus, combustion reaction was completed within a few minutes. The foam was then transferred in an agate mortar with a pestle to obtain fine particles. The combustion reaction for the synthesis of $CaAl_2O_4$-I by the redox mixture method (urea) can be written as:

$$3Ca(NO_3)_2 + 6Al(NO_3)_3 + 20NH_2CONH_2 \rightarrow 3CaAl_2O_4 + 20CO_2 + 40H_2O + 32N_2$$

The equivalance ratio (ϕ_e) in the above case is calculated as follows:

OV of $Ca(NO_3)_2$, 1Ca = +2, 2N =0, 6O = –12, Total = +2 –12 = –10.

RV of NH_2CONH_2, 1C = +4, 4H = +4, 2N = 0, 1O = –2, Total = +4+4–2 = +6.

(ϕ_e, *O/F)* = 10/6 = 1.66 *i.e.,* for every one mole of $Ca(NO_3)_2$ 1.66 moles of urea required.

OV of $Al(NO_3)_3$, 1Al = +3, 3N = 0, 9O = –18, Total = +3 –18 = –15.

RV of NH_2CONH_2, 1C = +4, 4H = +4, 2N = 0, 1O = –2, Total = +4+4–2 = +6.

(ϕ_e, *O/F)* = 15/6 = 2.5 *i.e.,* for every one mole of $Al(NO_3)_3$ 2.5 moles of urea required.

For the synthesis of $CaAl_2O_4$-I the total number of moles of urea required is: 1.66+2.5 = 4.16 mole.

Table 1. Stoicheometric proportion used for the synthesis of $CaAl_2O_4$-I

Mass of $Ca(NO_3)_2$ 4 H_2O	Mass of $Al(NO_3)_3$ 9 H_2O	Mass of NH_2CONH_2	Mass of Synthesized $CaAl_2O_4$-I
3.54g	11.255g	24g	2.98g

Photo1.

2.2.2 Synthesis of $CaAl_2O_4$-II

The stoichiometric amounts of $Ca(NO_3)_2.4H_2O$ (6.49g) and $Al(NO_3)_3.9H_2O$ (20.63g) were dissolved in a minimum quantity of water along with acetamide (5.90g) in a silica crucible (with a volume of 100 cm^3). The resulting mixture was introduced into the muffle furnace which was preheated to 600°C. Initially the solution foils boils and undergoes dehydration followed by decomposition with the evolution of gases (N_2 and CO_2). Then, it burns to yield voluminous and foamy homogeneous residue (Nesaraj *et al.* 2007). Thus, combustion reaction was completed within a few minutes. The foam was then lightly ground in an agate mortar with a pestle to obtain fine particles. The combustion reaction for the synthesis of $CaAl_2O_4$-II by the redox mixture method (acetamide) can be written as:

$$11Ca(NO_3)_2 + 22(Al(NO_3)_3 + 40CH_3CONH_2 \rightarrow 11CaAl_2O_4 + 80CO_2 + 100H_2O + 64\ N_2$$

The equivalance ratio (ϕ_e) in the above case is calculated as follows:

OV of $Ca(NO_3)_2$, 1Ca = +2, 2N = 0, 6O = –12, Total = +2 –12 = –10.

RV of CH_3CONH_2, 2C = +8, 5H = +5, 2N = 0, 1O = –2, Total = +8+5–2 = +11.

(ϕ_e, *O/F)* = 10/11 = 0.909 *i.e.,* for every one mole of $Ca(NO_3)_2$,0.909 mole acetamide required.

OV of $Al(NO_3)_3$, 1Al = +3, 3N = 0, 9O = –18, Total = +3 –18 = –15.

RV of CH_3CONH_2, 2C = +8, 5H = +5, 2N = 0, 1O = –2, Total = +8+5–2 = +11.

(ϕ_e *O/F)* = 15/11 = 1.36 *i.e.,* for every one mole of $Al(NO_3)_3$,1.36 mole acetamide required.

For the synthesis of $CaAl_2O_4$-II the total number of moles of acetamide required is: 0.909+1.36= 2.269 mole.

.**Table 2. Stoicheometric proportion used for the synthesis of $CaAl_2O_4$-II**

Mass of $Ca(NO_3)_2$ 4 H_2O	Mass of $Al(NO_3)_3$ 9 H_2O	Mass ofCH_3CONH_2	Mass of Synthesized $CaAl_2O_4$-II
6.49g	20.63g	5.90 g	4.34g

Photo 2: Synthesized $CaAl_2O_4$-II at 600 °C

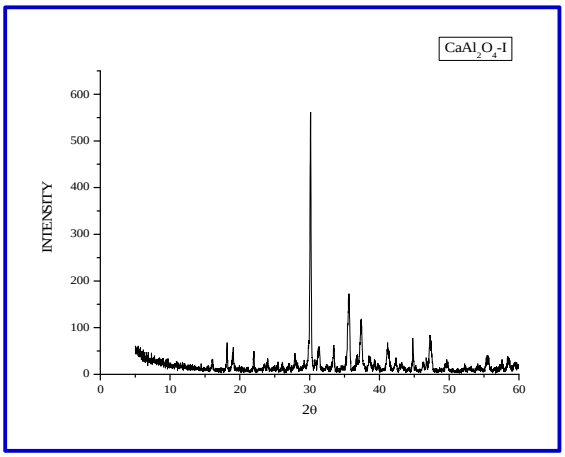

Fig. 1: X-ray diffraction of $CaAl_2O_4$-I

2.3 X-ray diffraction (XRD)

The powdered sample of $CaAl_2O_4$-I and $CaAl_2O_4$-II nano particles were examined by XRD and analysis was carried out on fresh sample to assess the purity of the expected phases and the degree of crystallization i.e., size, composition and crystal structure. XRD was performed by Rigakudiffractometer using Cu-K_α radiation (1.5406 Å) in a θ-2θ configuration (Girase *et al.* 2011). According to the Debye Scherrer's formula:

Debye Scherrer' formula $D= (K\lambda/\beta \cos \theta)$ … (Eq.1)

Where D = Thickness of the crystallite
K = 0.90 the Scherrer's constant (dependent on crystallite shape)
λ = X-ray wavelength
β = the peak width at half-maximum (FWHM)
θ = the Bragg diffraction angle

2.3.1 X-ray diffraction studies of $CaAl_2O_4$-I

The powdered sample of $CaAl_2O_4$-I nano particle was examined by XRD and analysis was carried out on fresh sample to assess the purity of the expected phases and the degree of crystallization *i.e.*, size, composition and crystal structure. XRD was performed by Rigakudiffractometer using Cu-K_α radiation (1.5406 Å) in a θ-2θ configuration

According to the XRD the average crystallite size of $CaAl_2O_4$-I was found to be 39 nm.

2.3.2 X-ray diffraction studies of $CaAl_2O_4$-II

The powdered sample of $CaAl_2O_4$-II nano particle was examined by XRD and analysis was carried out on fresh sample to assess the purity of the expected phases and the degree of crystallization *i.e.*, size, composition and crystal structure. XRD was performed by Rigakudiffractometer using Cu-K_α radiation (1.5406 Å) in a θ-2θ configuration. According to the XRD the average crystallite size of $CaAl_2O_4$-II was found to be 42 nm.

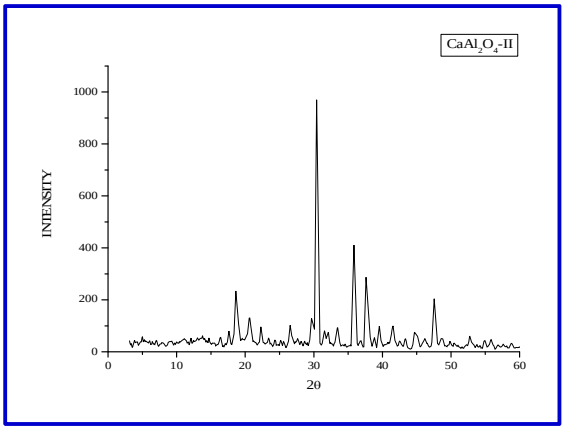

Fig. 2: X-ray diffraction of $CaAl_2O_4$-II

2.4 Scanning Electron Micrograph (SEM)

In the present work powdered sample of $CaAl_2O_4$-I and $CaAl_2O_4$-II nano particles were examined by using SEM technique. The study of the surface of the nano particle gives valuable information about its internal structure.

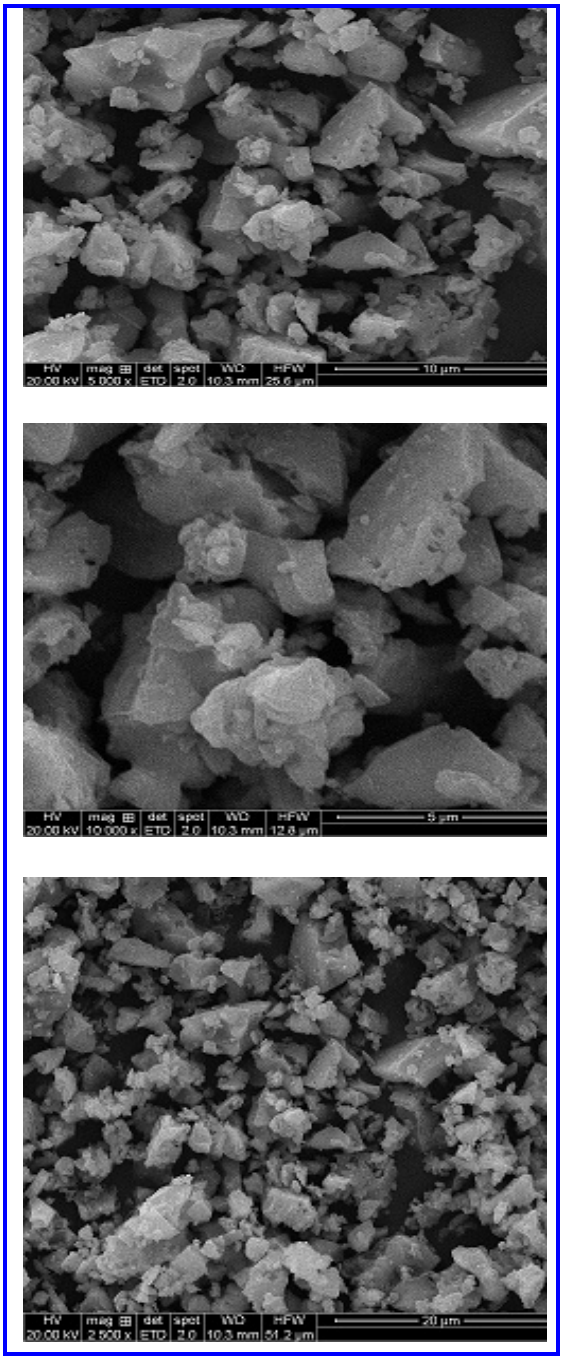

Fig. 3: SEM photograph of $CaAl_2O_4$-I

2.4.1 SEM study of $CaAl_2O_4$-I

The SEM photograph shows crystal morphology which are tightly packed. The overlapping of the crystals can be clearly observed in the images. The enlarged image shows the particles are attached to each other (Fig. 3).

2.4.2 SEM study of $CaAl_2O_4$-II

The SEM study shows both the mixtures of crystal and plate like morphology, which are placed at irregular interval. Here both small and large plates can be observed. The large individual plates can be seen with the sharp edged structures (Fig. 4).

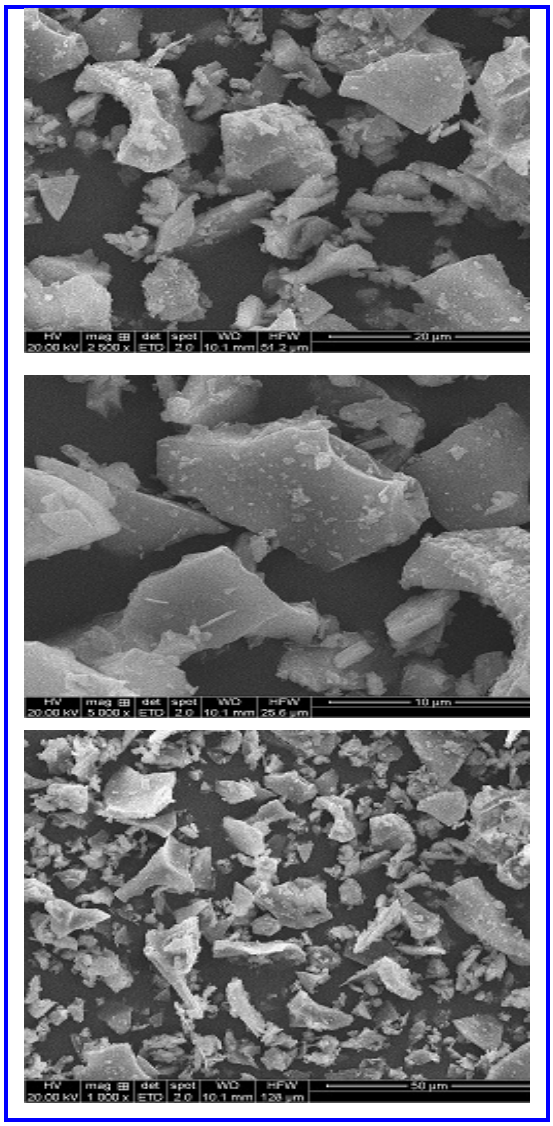

Fig. 4: SEM photograph of $CaAl_2O_4$-II

2.5 UV-absorption spectroscopy

Absorption spectra of the $CaAl_2O_4$-I and $CaAl_2O_4$-II metal oxide nano particles were recorded using UV-VIS spectrophotometer (Ocean Optics DH-2000) over the wavelength range 200-1200 nm at Nano Research Laboratory, Department of Nanotechnology, Kuvempu University. From this spectrum, it has been inferred that the nano particles have sufficient transmission in the entire visible and IR region. The band gap energy of the $CaAl_2O_4$-I and $CaAl_2O_4$-II nano particles was calculated using the following simple conversion equation. The band gap equation is calculated using the Planck's equation as follows.

$$E=hC/\lambda$$

h= Planck's constant, C= Velocity of light (speed of light), λ=wavelength of light

$h=4.135\times 10^{-15}$ eV, $C= 3\times10^{8}$ m/s, $\lambda=$ ---------$\times 10^{-9}$ nm

Band gap energy (eV) = 4.135×10^{-15} eV $\times 3 \times 10^{8} \times 10^{9}$

Band gap energy (eV) = (1240/ wavelength (nm)) …….. (Eq.2)

2.5.1 UV absorption study of $CaAl_2O_4$-I

Table 3. Band gap energy of $CaAl_2O_4$-I nano particle

Nano particle	λ_{max}(nm)	Band gap Energy (eV)
$CaAl_2O_4$-I	440	2.8

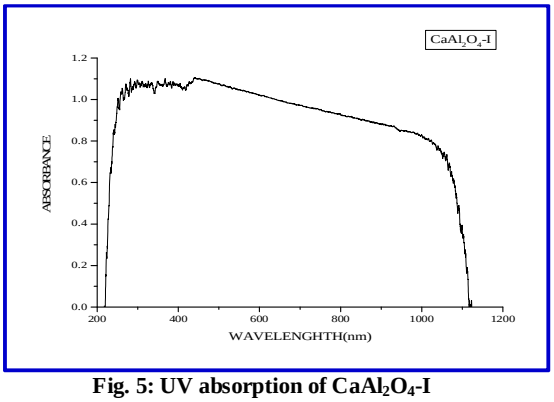

Fig. 5: UV absorption of $CaAl_2O_4$-I

Table 4. Band gap energy of $CaAl_2O_4$-II nano particle

Nano particle	λ_{max}(nm)	Band gap Energy (eV)
$CaAl_2O_4$-II	444	2.7

2.5.2 UV absorption study of $CaAl_2O_4$-II

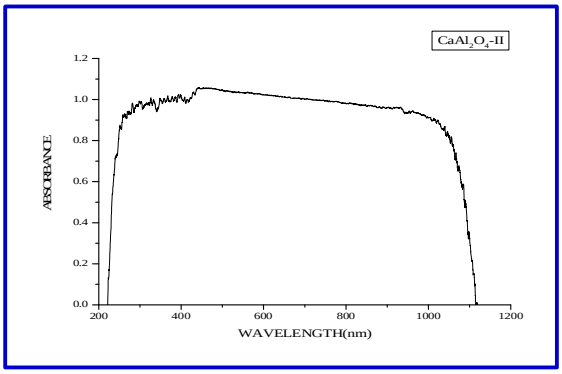

Fig. 6: UV absorption of $CaAl_2O_4$-II

The band gap energy of $CaAl_2O_4$-I is found to be 2.8 eV and $CaAl_2O_4$-II is found to be 2.7 eV. With this we can say that the band gap of the semiconductors has been found to be particle size dependent (Sawant *et al*. 2011).

3. RESULT & DISCUSSION

3.1 Photocatalytic experimental procedure: Initial study of the textile effluent

Raw wastewater sample was collected from homogeneous tank of the textile industry. Initially, sample was analyzed for some primary parameters like pH, Temperature, Odour, Colour, and COD. As the collected textile wastewater was highly concentrated, the sample was diluted with potable water before photocatalytic decolourization. The values of various wastewater parameters before treatment are shown in table 5.

Table 5. Characteristics of raw wastewater from textile industry

Sl. No.	Parameter	Value
1	pH	10.3
2	Temperature	36 °C
3	Odour	Unpleasant
4	COD	2202 mg/L
5	Colour	Black

3.2 Photocatalytic experimental procedure: Comparative study of photocatalytic decolourization of coloured textile effluent using the $CaAl_2O_4$-I and $CaAl_2O_4$-II nano particles over procured TiO_2

Photocatalytic experiments were carried out in presence of direct sunlight of intensity between

100000 to130000 lux (recorded by using TES 1332A digital Lux meter). The experiments were carried out between 10 am to 1 pm and 3ml of raw effluent was diluted 1000ml of potable water to make the aqueous solution of 3% concentration. In all photocatalytic experiments, 100ml of 3% textile effluent solution was taken in 100ml Borosil beakers. The UV-VIS spectrophotometer 119 (Systronics) was used for the determination of absorbance in the range of 200 to 800 nm. The λ_{max} of textile effluent was found to be 440 nm. A known amount of dosage (0.5 g/100 ml) of the different nano particles; TiO_2, $CaAl_2O_4$-I and $CaAl_2O_4$-II were added to six different beakers containing textile effluent solution and the beakers were kept in the sunlight for photocatalytic activity. Further experiments were conducted based on the decolourization results obtained from the photocatalytic activity of the catalysts.

3.3 Effect of photocatalysts on photocatalytic decolourization of textile effluent

Blank experiments were performed under direct sunlight without the addition of catalysts and no decolourization was observed. A known concentration of TiO_2, $CaAl_2O_4$-I and $CaAl_2O_4$-II (0.5 g/100 ml) were added to six beakers containing textile effluent solution and kept in the sunlight for photocatalytic activity. The results showed that the nano particles ($CaAl_2O_4$-I and $CaAl_2O_4$-II) have exhibited higher photocatalytic activity than TiO_2.

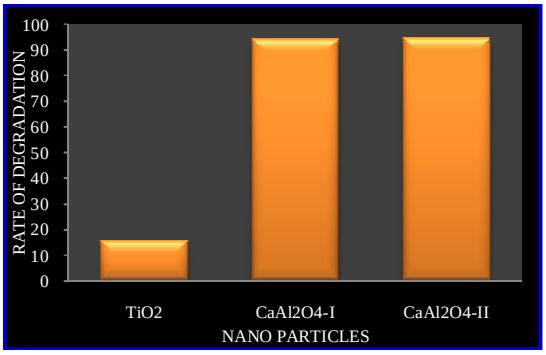

Fig. 7: Rate of degradation of textile effluent at 120 minutes [textile effluent =3%, pH=7, TiO_2=0.5g, $CaAl_2O_4$-I=0.5g, $CaAl_2O_4$-II=0.5g]

A decolourization of 15.60% was recorded for TiO_2 nano particle and 93.99% for $CaAl_2O_4$-I and 94.51% for $CaAl_2O_4$-II were recorded (Fig. 7) (Photo 3). Both the synthesized nano particles have exhibited higher photocatalytic activity than the commercially available TiO_2. Photocatalytic decolourization of the azo dye is mainly due to the hydroxyl radical attack on the dye molecule (Giwa *et al.* 2012). The production of hydroxyl radicals of the TiO_2 catalyst may be very less when compared with the synthesized nano particles which have exhibited high degradation in presence of sunlight. Based on the results further studies were done concentrating on the synthesized $CaAl_2O_4$-I and $CaAl_2O_4$-II nano particles.

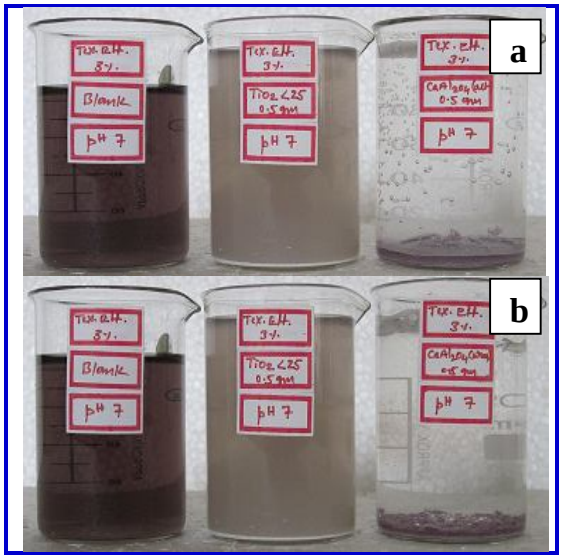

Photo 3: Rate of degradation of textile effluent at 120 minutes [(a)= textile effluent/TiO_2/$CaAl_2O_4$-I, (b)= textile effluent/TiO_2/$CaAl_2O_4$-II]

3.4 Photocatalytic experimental procedure: Study on photocatalyticdecolourization of textile effluent using $CaAl_2O_4$-I and $CaAl_2O_4$-II nano particles

In the second phase, the synthesized nano particles were continued for the photocatalytic degradation studies. Photocatalytic suspensions from 0.1g, 0.2g, 0.3g upto 1g were tested on the 100 ml textile effluent samples. The suspension pH values were adjusted by using NaOH/HCl solutions using pH meter. Before irradiation, photocatalyst suspension was stirred in the dark to ensure the adsorption equilibrium and was kept in sunlight for the photocatalyticdecolourization. At an interval of 30 minutes the suspension was sampled and centrifuged (EBA-Hetlich) at 3000rpm for 5 minutes to remove photocatalyst particles. The residual concentration of the solution samples were monitored by using UV-VIS spectrophotometer 119 (Systronics) at 440 nm. The experiments were conducted for different pH range from 2 to 11 in order to study the efficiency of the nano particles in Acidic, Alkaline and Neutral conditions. The data obtained from the photocatalytic degradation experiments were used to calculate the degradation efficiency 'D' (Eq. 3).

$$D = (A_0 - A_t / A_0) \times 100 \quad \text{..... (Eq. 3)}$$

where, A_0 is the initial absorbance of dye solution A_t is absorbance at time't'.

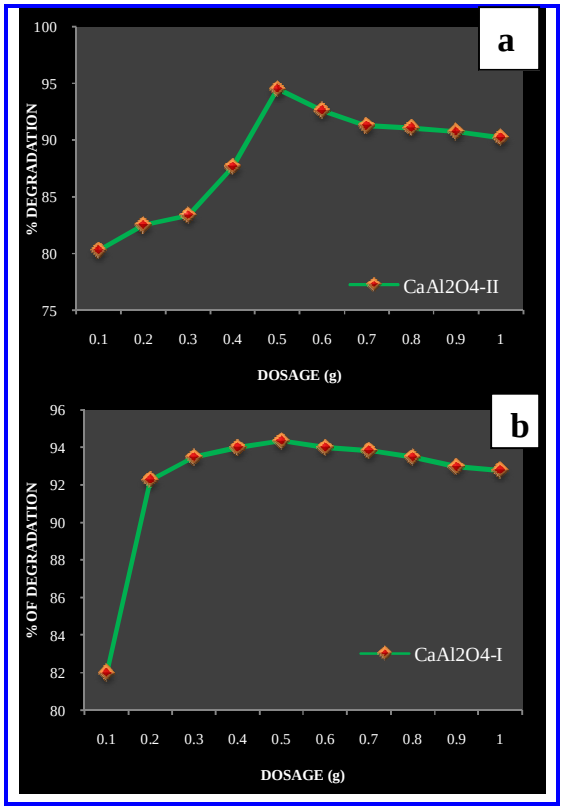

Fig. 8: Effect of catalyst concentration on textile effluent at 120 minutes [textile effluent=3 % at pH=7, (a)=$CaAl_2O_4$-I, (b)=$CaAl_2O_4$-II,]

3.5 Effect of catalyst concentration on textile effluent

The effect of catalyst concentration on photocatalytic degradation was studied over a range of catalyst amount from 0.1 to 1 g/100 ml for the textile effluent. Both the synthesized nano particles have shown appreciable results. Where, $CaAl_2O_4$-I showed 93.99 % at 0.4 g/100 ml and $CaAl_2O_4$-II showed highest degradation of 94.51 % at 0.5 g /100 ml in 120 minutes (Fig. 8) (Photo 4). The increase in decolourization rate can be explained in terms of availability of active sites on the catalyst surface and sunlight penetration into the suspension as a result of increased screening effect and scattering of light. Further increase in the catalyst amount beyond the optimum dosage for all the nano particles, decreases the decolourization by some margin. This may be due to overlapping of adsorption sites as a result of overcrowding owing to collision with ground state catalyst (Subramani *et al.* 2007). Since the decolourization was most effective at 0.6g/100ml for $CaAl_2O_4$-I and 0.7 g/100 ml for $CaAl_2O_4$-II nano particle dosages, the following experiments were continued with same dosages.

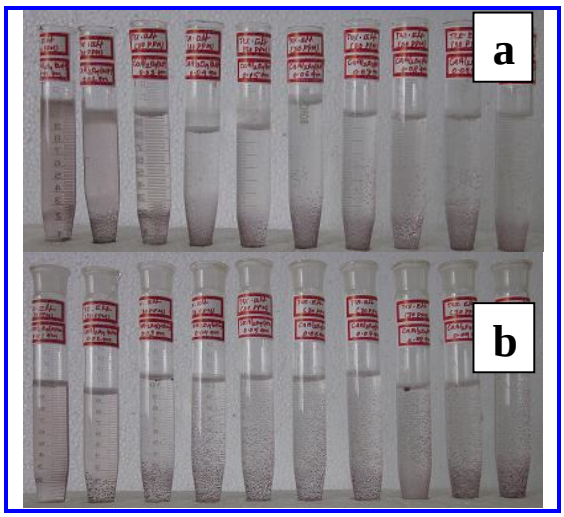

Photo 4: Effect of catalyst concentration on textile effluent at 120 minutes [textile effluent=3% at pH=7, (a)=$CaAl_2O_4$-I, (b)=$CaAl_2O_4$-II]

3.6 Mechanism of the photocatalytic decolourization

Nano particles+ hν → (e^-_{CB} + h^+_{VB}) (Eq. 4)

$e^-_{CB} + O_2 \rightarrow O_2^{\bullet -}$ (Eq. 5)

$H_2O + O_2^{\bullet -} \rightarrow OOH^{\bullet} + OH^-$ (Eq. 6)

$2OOH^{\bullet} \rightarrow O_2 + H_2O_2$ (Eq. 7)

$O_2^{\bullet -}$ + textile effluent → textile effluent -$OO^{\bullet}$ (Eq. 8)

$OOH^{\bullet} + H_2O + e^-_{CB} \rightarrow H_2O_2 + OH^-$ (Eq. 9)

$H_2O_2 + e^-_{CB} \rightarrow OH^{\bullet} + OH^-$ (Eq. 10)

$H_2O_2 + O_2^{\bullet -} \rightarrow OH^{\bullet} + OH^- + O_2$ (Eq. 11)

$OH^{\bullet}/O_2^{\bullet -}$/Nano particles$^{\bullet +}$ + textile effluent → textile effluent decolourization (Eq. 12)

The mechanism of photocatalytic activity of the used catalyst nano particle is predicted as follows.Under sunlight irradiation catalyst molecules get excited and transfer electron to the conduction band (Eq. 4). Electron in the conduction band of the catalyst can reduce molecular oxygen and produce the super oxide radical (Eq. 5). Molecular oxygen, adsorbed on the surface of the photocatalyst prevents the hole-electron pair recombination process (Di-Paola *et al.* 2003; Da-Silva and Faria, 2003). Recombination of hole-electron pair decreases the rate of photocatalytic degradation. This radical may form hydrogen peroxide or organic peroxide in the presence of oxygen and organic molecule (Eq. 6, 7, 8). Hydrogen peroxide can be generated in another path

(Eq. 9). Hydrogen peroxide can form hydroxyl radicals which are powerful oxidizing agents (Eq. 10, 11). The radicals produced are capable of attacking textile effluent molecules and decolourize them (Eq. 12).

3.7 Effect of pH on textile effluent

In order to study the effect of pH on the decolourization efficiency of $CaAl_2O_4$-I and $CaAl_2O_4$-II catalysts, the experiments were conducted at pH ranging from 2 to 11. The results showed that, pH significantly affected the decolourization efficiency (Fig. 9) (Photo 5). The decolourization rate of textile effluent for $CaAl_2O_4$-I, the decolourization increased from 88.50 % to 95.02 % from pH 2 to 8 and decreased to 93.31 % at pH 11 in 120 minutes for 0.4 g/100 ml and for $CaAl_2O_4$-II the decolourization of the effluent increased from 93.31 % to 95.71 % from pH 2 to 9 and decreased to 92.96% at 11 in 120 minutes for 0.5 g/100 ml. The maximum decolourization rate for all different nano particles was achieved at pH 8 and 9. As the collected effluent maybe having the anionic dyes which results in more efficient formation of hydroxyl radicals in alkaline medium. Excess of hydroxyl anions increases the formation of $OH^{\bullet}$ radicals. These $OH^{\bullet}$radicals are the main oxidizing species responsible for photocatalytic decolourization (Noorjahan *et al.* 2003).

Above optimum pH, the decrease in decolourization efficiency can be explained on the basis of amphoteric nature of the catalysts. The catalyst surface becomes negatively charged for higher pH values, which causes the electrostatic repulsion between the catalyst and negatively charged dyes (Turchi *et al.* 1990).

Photo 5: Effect of pH on the photocatalytic degradation of textile effluent at 120 minutes [textile effluent =3%, (a)=$CaAl_2O_4$-I, (b)=$CaAl_2O_4$-II,]

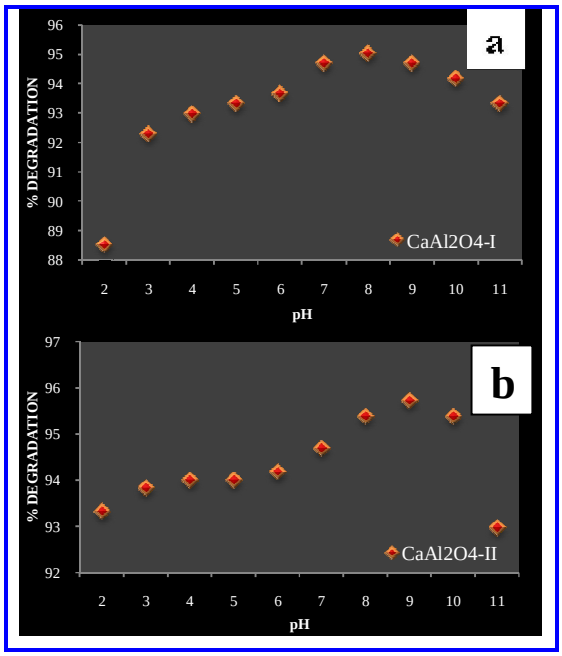

Fig. 9: Effect of pH on the photocatalytic degradation of textile effluent at 120 minutes [textile effluent = 3%, (a)=$CaAl_2O_4$-I, (b)=$CaAl_2O_4$-II,]

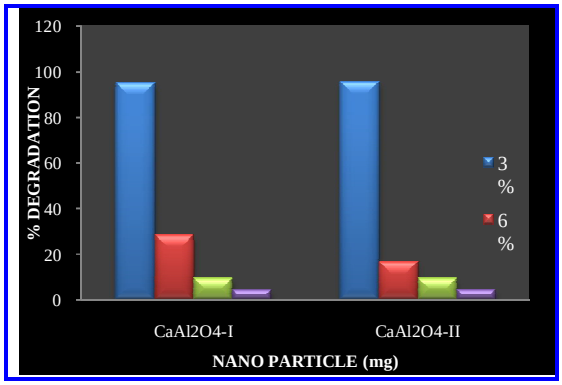

Fig. 10: Effect of initial dye concentration on photocatalytic degradation of textile effluent [(a)=$CaAl_2O_4$-I/pH=0.4g/8, (b)=$CaAl_2O_4$-II/pH=0.5g/9]

3.8 Effect on different concentration of textile effluent

The initial concentration of textile effluent was varied from 3%, 6%, 9% and 12% to study the effect on different concentrations of textile effluent. The decolourization results obtained for $CaAl_2O_4$-I obtained 95.02%, 28.49%, 9.56% and 4.56% for the aqueous solution 3%, 6%, 9% and 12%. In the same way $CaAl_2O_4$-II resulted 95.71%, 16.77%, 9.56% and 4.60% for the following 3%, 6%, 9% and 12% textile

effluent concentrations (Fig. 10) (Photo 6). These series of experiments illustrated that the decolourization efficiency was inversely affected by the concentration. The decrease in the decolourization with increase in effluent concentration was ascribed to the equilibrium adsorption of dye on the catalyst surface which results in decrease in the active sites. This phenomenon results in the lower formation of $OH^{\bullet}$ radicals which were considered as primary oxidizing agents of the organic dye (Mirkhani *et al.* 2009). According to Beer Lambert law, as the initial dye concentration increases, the path length of photons entering the solution decreases. This results in lower photon adsorption on the catalyst particles, and consequently decreases photocatalytic reaction rate (Byrappa *et al.* 2006).

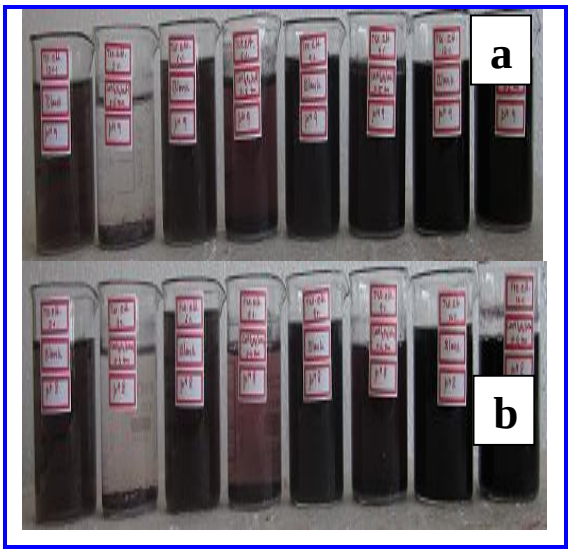

Photo 6: Effect of initial dye concentration on photocatalytic degradation of textile effluent [(a)=$CaAl_2O_4$-I/pH= 0.4g/8, (b)=$CaAl_2O_4$-II/pH= 0.5g/9]

3.9 Effect of sunlight irradiation on textile effluent

Sunlight irradiation generates the photons required for the electron transfer from the valence band to the conduction band of a semiconductor photocatalyst. The energy of a photon is related to its wavelength and the overall energy input to a photocatalytic process is dependent on the light intensity. Therefore, the effects of both intensity and wavelength are important. In the present study, the effect of the sunlight intensity was studied by keeping the constant wavelength (440 nm).

The The photocatalytic decolourization of diluted textile effluent (*i.e.* 3%) conducted under three different experimental conditions were examined, *i.e.*, under sunlight alone, textile effluent/dark/catalyst and textile effluent/sunlight/catalyst for both the different catalysts. When textile effluent solution was exposed directly to the sunlight, the decolourization was found to be nil during the entire experiments.

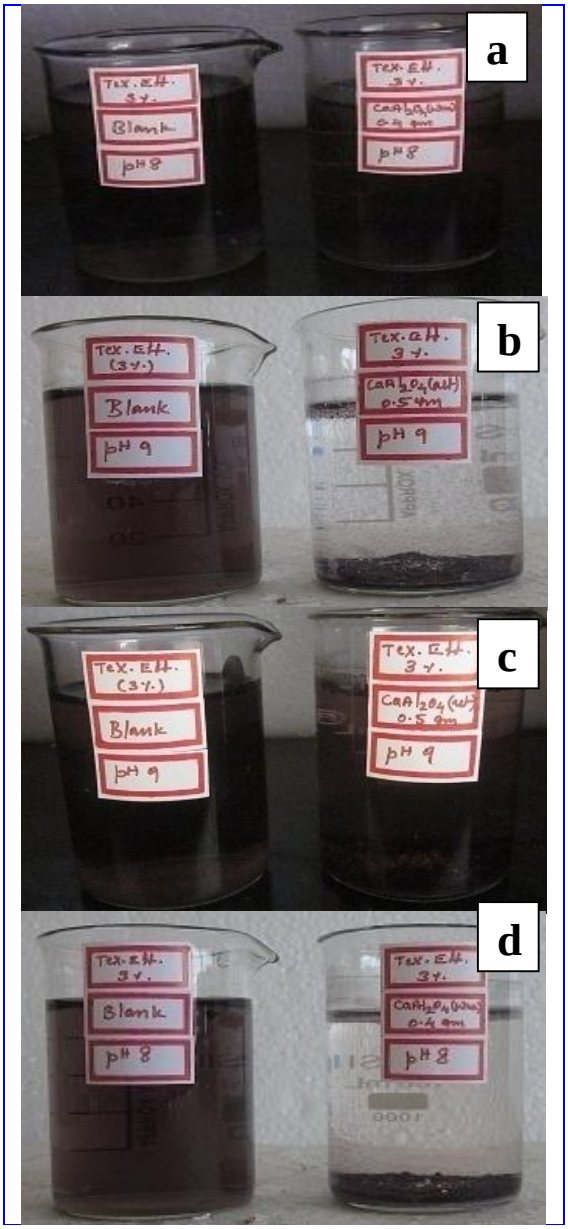

Photo 7: Effect of sunlight irradiation on photocatalytic degradation of textile effluent in 120 minutes. [(a)= textile effluent/sunlight/$CaAl_2O_4$-I at pH 8, (b)= textile effluent/sunlight/$CaAl_2O_4$-II at pH 9] [(a1)= textile effluent/dark/$CaAl_2O_4$-I at pH 8, (b1)= textile effluent/dark/$CaAl_2O_4$-II at pH 9]

The decolourization rate was found to increase with increase in irradiation time, for textile effluent/sunlight/$CaAl_2O_4$-I recorded 95.02% and textile effluent/dark/ $CaAl_2O_4$-I 16.29% was recorded. The textile effluent/sunlight/$CaAl_2O_4$-II achieved 95.71 % and textile effluent/dark/$CaAl_2O_4$-II 27.27 % was recorded with 120 minutes respectively (Fig. 11) (Photo 7). These results clearly showed that, decolourization occurs more efficiently in presence of sunlight. Under sunlight excitation of catalysts takes place rapidly than in absence of light. The experiment demonstrated that, both sunlight and photocatalyst are needed for the effective destruction of textile effluent, as it has been established that the photocatalytic decolourization of organic matter in the effluent is initiated by the photo excitation of the semiconductor, followed by the formation of electron hole pair on the surface of the catalyst.

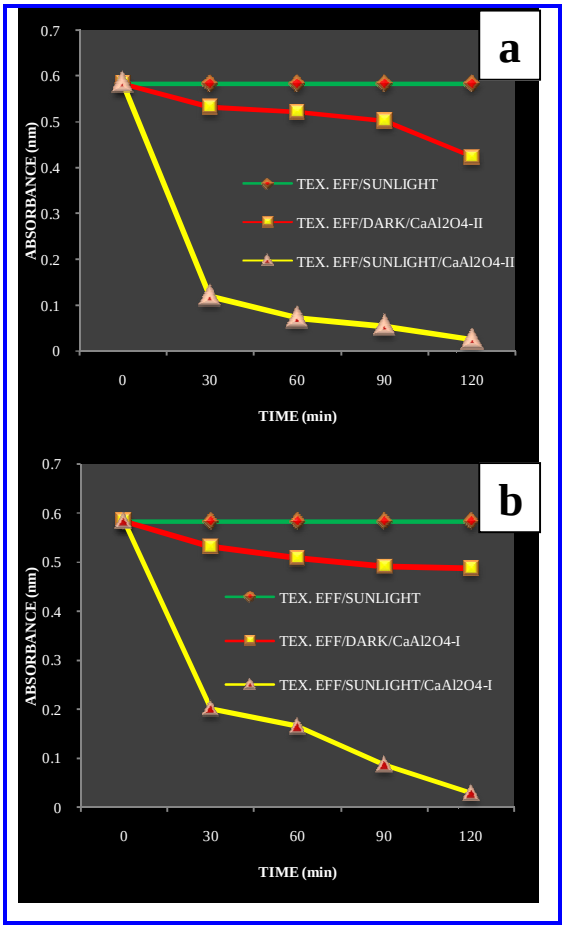

Fig. 11: Effect of sunlight irradiation on photocatalytic degradation of textile effluent in 120 minutes. [(a)=$CaAl_2O_4$-I at pH 8, (b)=$CaAl_2O_4$-II at pH 9]

4. CONCLUSION

In the present work two photocatalysts were prepared by solution combustion method. $CaAl_2O_4$-I and $CaAl_2O_4$-II were characterized by different technique such as XRD, SEM and UV-Vis reflectance. The coloured textile effluent is undesirable for the aquatic environment as it limits the utilization of the water resources. Photocatalytic decolorization is an alternative method to other conventional inefficient physico-chemical and biological methods to treat toxic effluents. The feasibility of photocatalytic decolourization and degradation of the effluent was studied by using the synthesized metal oxide nano particles as photocatalysts.

The synthesized photocatalysts have shown a maximum decolourization of the selected effluent under solar radiation. Among the catalysts used except TiO_2 all the other nano particles $CaAl_2O_4$-I and $CaAl_2O_4$-II were proved to be very efficient photocatalysts in decolorizing the azo dye and achieving 93.99 % and 94.51 % respectively in 120 minutes at pH 7. The synthesized nano particles have been more efficient than the procured nano particle TiO_2 which could able to achieve only 15.60 % of decolourization in 120 minutes at pH 7.

Similarly, when the pH was altered, 95.02% at pH 8 for 0.4 g/100 ml and 95.71 % at pH 9 for 0.5 g/100 ml to the following $CaAl_2O_4$-I and $CaAl_2O_4$-II metal oxide nano particles. Hence, the obtained results have proved that, photocatalytic decolourization of textile effluent was mainly dependent on the pH of the dye solution and catalyst dosage. The textile effluent achieved high colour removal in alkaline medium. The results also revealed that, the sunlight is the most efficient source for photocatalytic activity and the used nano particle is an effective media to decolorize the coloured effluents.

ACKNOWLEDGEMENT

The authors would like to acknowledge their sincere thanks to University Grants Commission, New Delhi for the financial assistance in conducting the present research work.

REFERENCES

Behnajady, A., Modirshahla, N. and Hamzavi, R., Kinetic study on photocatalytic degradation of C. I. Acid Yellow 23 by ZnO photocatalyst, *J. Hazard. Mater*., B, 133 (1-3), 226-232(2006).

Byrappa, K., Subramani, A. K., Ananda, S., LokanathaRai, K. M., Dinesh, R. and Yoshimura, M., Photocatalytic degradation of Rhodamine B dye using hydrothermally synthesized ZnO, *Bull. Mater. Sci.*, 29 (5), 433-438(2006). doi:10.1007/BF02914073

Da-Silva, C. G., and Faria, J. L., Photochemical and photocatalytic degradation of an azo dye in aqueous solution by UV irradiation, *J. Photochem. Photobiol.*, A, 155 (1-3), 133-143(2003).

Deshpande, K., Mukasyan, A. M. and Varma, A., Direct synthesis of iron oxide nano powders by the combustion approach: reaction mechanism and properties, *Chem. Mater.*, 16 (24), 4896-4904(2004). doi:10.1021/cm040061m

Di-Paola, A., Augugliaro, V., Palmisano, L., Pantaleo, G. and Savinov, E., Heterogeneous photocatalytic degradation of nitrophenols, *J. Photochem. Photobiol.*, A, 155 (1-3), 207-214(2003).

Girase, K. D., Patil, H. M., Sawant, D. K. and Bhavsar, D. S., Effect of Cu2+ Doping on the Growth and Band Gap Energy of Nano Crystals of Lead Iodate, *Arch. Appl. Sci. Res.*, 3 (3), 128–134(2011).

Giwa, A., Nkeonye, P. O., Bello, K. A., Kolawole, E. G. and Oliveira Campos, A. M. F., Solar Photocatalytic Degradation of Reactive Yellow 81 and Reactive Violet 1 in Aqueous Solution Containing Semiconductor Oxides, *Int. J. Appl. Sci. Technol.*, 2 (4), 90-105(2012).

Gopalappa, H., Yogendra, K., Mahadevan, K. M. and Madhusudhana, N., A comparative study on the solar photocatalytic degradation of Brilliant red azo dye by CaO and CaMgO2 nano particles, *Int. J. Sci. Res.*, 1 (2), 91-95(2012).

Gopalappa, H., Yogendra, K., Mahadevan, K. M. and Madhusudhana, N., Solar Photocatalytic degradation of Orange G (mono azo dye) and C. I. Direct Yellow 50 (di azo dye) by synthesized CaZnO2 nano particle in aqueous solution, *Int. J. Univ. Pharm. Life Sci.*, 2 (4), 66-77(2012).

Gouvea, C. A. K., Wypych, F., Moraes, S. G., Duran, N., Nagata, N. and Peralta-Zamora, P., Semiconductor-assisted photocatalytic degradation of reactive dyes in aqueous solution, *Chemosphere*, 40 (4), 433-440(2000). doi:10.1016/S0045-6535(99)00313-6

Khodja, A. A., Sehili, T., Pilichowski, J. F. and Boule, P., Photocatalytic degradation of 2-phenylphenol on TiO_2 and ZnO in aqueous suspensions, *J. Photochem. Photobiol., A*, 141 (2-3), 231-239(2001).

Lizama, C., Freer, J., Baeza, J. and Mansilla, H. D., Optimized photodegradation of reactive Blue 19 on TiO_2 and ZnO suspensions, *Catal. Today*, 76 (2-4), 235-246(2002). doi:10.1016/S0920-5861(02)00222-5

Madhusudhana, N., Yogendra, K. and Mahadevan, K. M., A comparative study on Photocatalytic degradation of Violet GL2B azo dye using CaO and TiO_2 nano particles, *Int. J. Eng. Res. Appl.*, 2 (5), 1300-1307(2012).

Madhusudhana, N., Yogendra, K. and Mahadevan, K. M., Photocatalytic degradation of Violet GL2B azo dye by using Calcium aluminate nano particle in presence of solarlight, *Res. J. Chem. Sci.*, 2 (5), 72-77(2012).

Madhusudhana, N., Yogendra, K. and Mahadevan, K. M., Photocatalytic Decolourization of Textile Effluent by Using Metal Oxide Nano particles, *J. Sci. Arts*, 3 (24), 303-318(2013).

Madhusudhana, N., Yogendra, K., Mahadevan, K. M., and SuneelNaik, Photocatalytic degradation of Coralene Dark Red 2B azo dye using Calcium zincate as an nano particle in presence of natural sunlight: An aid to environmental remediation, *Int. J. Chem. Eng. Appl.*, 2 (4), 301-305(2011).

Malato, S., Blanco, J., Vidal, A. and Richter, C., Photocatalysis with solar energy at a pilot-plant scale: an overview, *Appl. Catal., B*, 37 (1), 1-15(2002). doi:10.1016/S0926-3373(01)00315-0

Manjusha, K. and Pragati, T., Photocatalytic Degradation and Mineralization of Reactive Textile Azo Dye Using Semiconductor Metal Oxide Nano Particles, *Int. J. Eng. Res. Gen. Sci.*, 2 (2), 245-254(2014).

Mimani, T. and Patil, K.C., Solution combustion synthesis of nanoscale oxides and their composites, *Mater. Phy. Mech.*, 4 (1), 134-137(2001).

Mirkhani, V., Tangestaninejad, S., Moghadam, M., Habibi, M. H. and Rostami Vartooni, A., Photocatalytic Degradation of Azo Dyes Catalyzed by Ag Doped TiO_2 Photocatalyst, *J. Iranian Chem. Soc.*, 6 (3), 578-587(2009). doi:10.1007/BF03246537

Mohammad, H. H., Ali, H. and Mahdavi, S., The effect of operational parameters on the photocatalytic degradation of three textile azo dyes in aqueous TiO_2 suspensions, *J. Photochem. Photobiol., A*, 172 (1), 89-96(2005).

Nesaraj, A. S., Arul Raj, I. and Pattabiraman, R., Synthesis and characterization of $LaCoO_3$ based cathode and its chemical compatibility with CeO_2 based electrolytes for Intermediate Temperature Solid Oxide Fuel Cell (ITSOFC), *Indian J. Chem. Technol.*, 14 (1), 154-160(2007).

Noorjahan, M., Pratap Reddy, M., DurgaKumari, V., Lavedrine, B., Boule, P. and Subrahmanyam, M., Photocatalytic degradation of H-acid over a novel TiO_2 thin film fixed bed reactor and in aqueous suspensions, *J. Photochem. Photobiol., A*, 156 (1-3), 179-187 (2003).

Sawant, D. K., Patil, H. M., Bhavsar, D. S., Patil, J. H. and Girase, K. D., Structural and Optical Properties of Calcium Cadmium Tartrate, *Arch. Phys. Res.*, 2, 67-73 (2011).

Subramani, A. K., Byrappa, K., Ananda, S., LokanathaRai, K. M., Ranganathaiah, C. and Yoshimura, M., Photocatalytic degradation of indigo carmine dye using TiO_2 impregnated activated carbon, *Bull. Mater. Sci.*, 30 (1): 37-41 (2007). doi:10.1007/s12034-007-0007-8

Swati., Munesh. and Meena, R. C., Photocatalytic degradation of textile dye through an alternative photocatalyst methylene blue immobilized resin dowex 11 in presence of solar light, *Arch. Appl. Sci. Res.*, 4 (1), 472-479 (2012).

Turchi, C. S. and Ollis, D. F., Photocatalytic Degradation of Organic Water Contaminants: Mechanisms Involving Hydroxyl Radical Attack, *J. Catal.*, 122 (1), 178-192 (1990). doi:10.1016/0021-9517(90)90269-P

Yeber, M. C., Rodriguez, J., Freer, J., Duran, N. and Mansilla, H. D., Photocatalytic degradation of cellulose bleaching effluent by supported TiO_2 and ZnO, *Chemosphere*, 41 (8), 1193-1197 (2000). doi:10.1016/S0045-6535(99)00551-2

Yogendra, K., Suneel Naik, Mahadevan, K. M., and Madhusudhana, N., A comparative study of photocatalytic activities of two different synthesized ZnO composites against Coralene Red F3BS dye in presence of natural solar light, *Int. J. Environ. Sci. Res.*, 1 (1), 11-15 (2011).